Original Paper

Cells Tissues Organs

Cells Tissues Organs
DOI: 10.1159/000353218

Accepted after revision: May 21, 2013
Published online: July 25, 2013

3-D Technology Used to Accurately Understand Equine Ileocolonic Aganglionosis

Eliane Muniz[a] Aliny A.B. Lobo Ladd[b] Fernando V. Lobo Ladd[b]
Andrea A.P. da Silva[b] Fernanda V. Kmit[b] Alexandre S. Borges[e]
Raffaella Teixeira[e] Lígia S.L.S. da Mota[e] Carla B. Belli[c] André L.V. de Zoppa[d]
Luis C.L.C. da Silva[d] Mariana P. de Melo[f] Antonio A. Coppi[b]

[a]Laboratory of Experimental Neurogastroenterology, Universidade Paranaense, Umuarama, [b]Laboratory of Stochastic Stereology and Chemical Anatomy, Department of Surgery, [c]Department of Internal Medicine, and [d]Department of Surgery, College of Veterinary Medicine and Animal Science, University of São Paulo, [e]Department of Veterinary Clinical Science, College of Veterinary Medicine and Animal Science, Universidade Estadual Paulista, Campus Botucatu, and [f]Department of Statistics, Institute of Mathematics and Statistics, University of São Paulo, São Paulo, Brazil

Key Words
Ileocolonic aganglionosis · Overo lethal white syndrome · Myenteric plexus · Submucosal plexus · Horses · Stereology

Abstract
Ileocolonic aganglionosis (ICA) is the congenital and hereditary absence of neurons that constitute the enteric nervous system and has been described in various species including humans – Hirschsprung's disease – and horses – overo lethal white syndrome (OLWS). Hirschsprung's disease affects circa 1 in 5,000 live births. At best, this disease means an inability to absorb nutrients from food (humans). At worse, in horses, it always means death. Despite our general understanding of the functional mechanisms underlying ICA, there is a paucity of reliable quantitative information about the structure of myenteric and submucosal neurons in healthy horses and there are no studies on horses with ICA. In light of these uncertainties, we have used design-based stereology to describe the 3-D structure – total number and true size – of myenteric and submucosal neurons in the ileum of ICA horses. Our study has shown that ICA affects all submucosal neurons and 99% of myenteric neurons. The remaining myenteric neurons (0.56%) atrophy immensely, i.e. 63.8%. We believe this study forms the basis for further research, assessing which subpopulation of myenteric neurons are affected by ileocolonic aganglionosis, and we would like to propose a new nomenclature to distinguish between a complete absence of neurons – aganglionosis – and a weaker form of the disease which we suggest naming 'hypoganglionosis'. Our results are a step forward in understanding this disease structurally.

Abbreviations used in this paper

CE	coefficient of error
CV	coefficient of variation
ICA	ileocolonic aganglionosis
OLWS	overo lethal white syndrome
SUR	systematic uniform random
VUR	vertical and uniform random

KARGER

E-Mail karger@karger.com
www.karger.com/cto

1422–6405/13/0000–0000$38.00/0

Prof. Antonio Augusto Coppi
Departamento de Cirurgia, Faculdade de Medicina Veterinária e Zootecnia
Universidade de São Paulo, Av. Prof. Dr. Orlando Marques de Paiva, 87
São Paulo, SP 05508-270 (Brazil)
E-Mail GUTO@USP.BR

Introduction

Intestinal aganglionosis is a congenital and hereditary absence of neurons that normally form the submucosal and myenteric ganglia. The neuron deficiency is associated with peristaltic disorders [Taniguchi et al., 2005] and has been described in various species including mice, horses and humans [McCabe et al., 1990; Nagahama et al., 2001]. In humans, this disturbance is known as Hirschsprung's disease [Taniguchi et al., 2005] and affects circa 1 in 5,000 live births [Santschi et al., 1998]. The naturally occurring horse variant of Hirschsprung's disease is known as ileocolonic aganglionosis (ICA) or overo lethal white syndrome (OLWS) [Brashier and Geor, 1995; Metallinos et al., 1998; Lightbody, 2002; Finno et al., 2009], which is a fatal condition, and foals die within the first few days after birth due to an obstruction-induced intestinal severe colic and paralytic ileum [McCabe et al., 1990; Parry, 2005]. In both horses and humans, aganglionosis results from a congenital disorder of neural crest cell migration throughout the intestine (craniocaudal migration theory) [Okamoto and Ueda, 1967; Santschi et al., 1998; Lightbody, 2002].

Despite our general understanding of the functional mechanisms underlying ICA, there is a paucity of reliable and accurate quantitative information about the structure of the myenteric and submucosal neurons in healthy horses, and there are no publications on the quantitative structure of neurons in horses with ICA. The problem with previous research – in healthy horses – has been the use of 2-D quantitative microscopy methods (membrane preparations) for assessing enteric neurons [Pearson, 1994; Doxey et al., 1995; Freytag et al., 2008]. After perusing the literature, surprisingly, we have not yet found any 3-D design-based stereological data on the enteric nervous system of healthy and ICA horses.

Hence, we have used cutting-edge 3-D technology – design-based stereology – to quantify aspects of the structure of the myenteric and submucosal neurons in healthy and ICA horses. We hope this study will be a step forward in understanding – from a structural point of view – the enteric nervous system of large animals and its related disorders.

Materials and Methods

Animals

The present study was approved by the Animal Care Committee of the School of Veterinary Medicine and Animal Science of the University of São Paulo and by the Research Ethics Committee of the Federal University of São Paulo. The experimental protocol approval references are: 1516/2008 and 1660/08. The ileum was removed from each of 10 male foals obtained from the Department of Veterinary Clinical Science, College of Veterinary Medicine and Animal Science in Botucatu, São Paulo, Brazil, and from the School of Veterinary Medicine and Animal Science of the University of São Paulo. According to the absence and presence of ICA, the horses were divided into two groups including 5 healthy (crossbreed foals) and 5 ICA (Paint Horse foals) cases, respectively. Animals were between 3 and 7 days old and the mean body weight was 40 kg (SD 2). Healthy horses had no gastrointestinal disorders and were euthanized in conjunction with other experiments.

Clinical Examination

All animals were examined for the possible presence of gastrointestinal disorders. ICA horses were examined within 4 h after birth and subsequently twice a day (for 3–6 days on average) in order to assess their clinical development. The following clinical parameters were investigated: respiratory and heart rates, body temperature and intestinal borborygmus.

Genetic Diagnosis of ICA

The clinical diagnosis of ICA was confirmed genetically. Blood sample DNA purification was performed using the GFX Genomic Blood DNA Purification Kit (Amersham Biosciences), following the manufacturer's instructions. PCR for DNA sequencing was performed slightly modified, as described by Metallinos [1998] and Schmittgen and Livak [2008]. The obtained PCR products were analysed via 1.5% agarose gel electrophoresis (Invitrogen, Carlsbad, Calif., USA), stained with the Sybr Safe DNA Gel Stain (Invitrogen) and then purified using the QIAquick PCR Purification Kit (Qiagen). The purified products were then submitted for direct sequence analysis using the MegaBACE 1000 Sequencing and DYEnamic ET Dye Terminator Kit (Amersham Biosciences, Sunnyvale, Calif., USA). Each reaction was performed in duplicate using 5 μl of each of the forward and reverse primers. The obtained sequences and electropherograms were analysed using Sequencher 4.7 (Gene Codes, Ann Arbor, Mich., USA).

Euthanasia and Histology

Animals were sedated with intramuscular azaperone (4 mg·kg^{-1}) followed by intramuscular atropine sulphate (0.06 mg·kg^{-1}). Anaesthesia involved a combination of 20 mg·kg^{-1} intramuscular ketamine chloride and 1.5 mg·kg^{-1} intramuscular xylazine hydrochloride and the euthanasia was conducted using an intravenous 100 mg·kg^{-1} overdose of thionembutal (Abbot).

Since the ileum is most severely affected by ICA in horses [Hultgren, 1982; Vonderfecht et al., 1983; Finno et al., 2009], this portion of the small intestine was selected for the stereological study.

After euthanasia, each ileum was dissected out, weighed, and its wet weight was converted into volume using a tissue density of 1.06 g·cm^{-3} [Weibel, 1979]. Fresh volumes were estimated in order to monitor tissue shrinkage distortion after processing. The length of each ileum was also measured using a digital pachymeter (Digimess) [Ogiolda et al., 1998]. Next, the ileum was immersion fixed with 4% formaldehyde in PBS (0.1 M, pH 7.4) for 24 h.

Following immersion fixation, each ileum was transversely sectioned into 3-cm-thick portions using a systematic uniform random (SUR) sampling scheme [Gundersen et al., 1999]. The num-

ber of portions for a given ileum depended on its length and on the group studied. For the healthy group, on average, 15 portions were generated. A sampling fraction of these portions (psf = 1/3) was chosen [Gundersen et al., 1999], as shown in figure 1. Using a tissue slicer, each of these 5 portions was then divided into ten 0.3-cm-thick rings and a sampling fraction of these rings (rsf = 1/5) was SUR selected obtaining 10 rings on average (fig. 1). Rings were next opened in order to expose their lumina, placed onto a horizontal surface and arranged into bars 8 cm in length (fig. 1). Next, a sampling fraction of these bars (bsf = 1/2) was SUR selected obtaining 5 bars on average (fig. 1). Subsequently, each bar was cut into 10 strips, on average, and arranged in order of increasing size using the smooth fractionator principle [Gundersen, 2002] (fig. 1). Next, a sampling fraction of these strips (ssf = 1/4) was SUR sampled. On average, 12 strips were obtained per ileum for embedding (for more details, see Embedding Procedures).

For the ICA group, on average, 12 ileum portions were generated. A sampling fraction of these portions (psf = 1/2) was chosen [Gundersen et al., 1999]. Using a tissue slicer, each of these 6 portions was then divided into ten 0.3-cm-thick rings, and a sampling fraction of these rings (rsf = 1/6) was SUR selected obtaining 10 rings on average. Rings were next opened in order to expose their lumina, placed onto a horizontal surface and arranged into bars 5 cm in length. Next, a sampling fraction of these bars (bsf = 1/2) was SUR selected obtaining 5 bars on average. Subsequently, each bar was cut into 7 strips (on average) and arranged in order of increasing size using the smooth fractionator principle [Gundersen, 2002]. Next, a sampling fraction of these strips (ssf = 1/4) was SUR sampled. On average, 8 strips were obtained per ileum for embedding (for more details, see Embedding Procedures).

Design-Based Stereology

Volume of Ileum

The total volume of each ileum was estimated by means of the Cavalieri principle [Gundersen et al., 1999; Howard and Reed, 2010] using the following formula:

$$V_{ILE} = psf^{-1} \cdot rsf^{-1} \cdot T \cdot \Sigma A_{ILE},$$

where V_{ILE} is the total volume of each ileum, T is the ring thickness (0.3 cm), psf and rsf are portion and ring sampling fractions, respectively (as described above for each group), and ΣA_{ILE} is the sum of the delineated profile areas of the sampled ileum rings. Profile areas were estimated using a test lattice of coarse and fine points (approximately 551 and 273 per ileum for the healthy and ICA groups, respectively). Areas were obtained from the numbers of randomly positioned test points hitting the whole reference space (lumen + wall) and the areal equivalent of a test point (0.072 cm^2 for the wall and 0.325 cm^2 for the lumen). Irrespective of the group, the mean volume shrinkage [coefficient of variation (CV), expressed as a decimal fraction of the mean] was estimated to be 9.3% (CV 0.21) for the healthy group and 6.6% (CV 0.20) for the ICA group. A correction for global shrinkage was performed since between-group differences were significant (p = 0.03).

Embedding Procedures

In order to produce vertical and uniform random (VUR) sections [Baddeley et al., 1986; Kissmeyer-Nielsen et al., 1994], ileum strips were rotated along their normal axis, and their vertical axes were marked using a Tissue Marking Dye System (Cancer Diagnostics, Inc., Birmingham, Ala., USA). Subsequently, specimens were washed in sodium cacodylate buffer, post-fixed in a buffered solution of 2% osmium tetroxide, stained en bloc with a saturated aqueous solution of uranyl acetate (Electron Microscopy Sciences, Hatfield, Pa., USA), dehydrated in graded ethanol concentrations and propylene oxide (Electron Microscopy Sciences) and embedded in Araldite 502 (Electron Microscopy Sciences). Araldite blocks of tissue were polymerized in the oven at 60–70°C for 3 days. For light microscopy, 2- and 0.6-μm-thick VUR sections were exhaustively cut with glass knives using a UC6 automatically calibrated Leica ultramicrotome (for more details, see Total Number of Neurons).

Next, sections were collected onto glass slides, dried on a hot plate, stained with toluidine blue and mounted onto a coverslip with a drop of Araldite. Section images were acquired using a DM6000 Leica microscope (Leica Microsystems, Wetzlar, Germany) equipped with a High-End DP 72 Olympus digital camera (Olympus, Essex, UK) and projected onto a flat-screen computer monitor. Stereological analyses were performed using the autodisector and the nucleator procedures of the newCAST Visiopharm stereology system version 4.4.4.0 (Visiopharm, Copenhagen, Denmark).

Total Number of Myenteric and Submucosal Neurons

The physical fractionator was used for estimating the total number of neurons of the myenteric and submucosal ganglia [Gundersen, 1986; Mayhew, 1991]. Each Araldite block was exhaustively serially sectioned into 2- and 0.6-μm-thick sections, and a sampling fraction (secsf = 1/1,728 and 1/2,318 for myenteric and submucosal neurons in the healthy group, respectively, and 1/840 for both myenteric and submucosal neurons in the ICA group) of those 'reference' sections was selected together with two companion 'look-up' sections, which were 0.6 μm (look-up 1 section) and 2.6 μm (look-up 2 section) distant from the reference sections. Look-up 1 sections were used for sampling the nucleolus and estimating neuron volume. Look-up 2 sections were used for sampling the perikaryon (soma) and estimating the total number of neurons. The disector height was 2.6 μm. An area sampling fraction – of 3.37 and 2.33 for myenteric and submucosal neurons in the healthy group, respectively, or 2.11 for both myenteric and submucosal neurons in the ICA group – of the chosen sections was sampled using 2-D unbiased counting frames with a frame area equivalent to 6,400 μm^2 [Gundersen, 1977]. The same sampled area was followed by 3 consecutive sections, i.e. one 2-μm-thick section followed by another 0.6-μm-thick section and one more 2-μm-thick section.

For the healthy group, an average of 356 disectors were used to count 144 myenteric neurons and 178 disectors to count 44 submucosal neurons (ΣQ^-). In the ICA group, 44 disectors were applied to count 3 myenteric neurons and 45 disectors were applied, though no submucosal neurons were found. The total number of myenteric or submucosal neurons was then estimated by multiplying the counted number of particles by the reciprocal of sampling fractions:

$$N_{mye/sub} = psf^{-1} \cdot rsf^{-1} \cdot bsf^{-1} \cdot ssf^{-1} \cdot secsf^{-1} \cdot asf^{-1} \cdot \Sigma Q^-/2,$$

where $N_{mye/sub}$ is the total number of myenteric and submucosal neurons, psf, rsf, bsf, ssf, secsf and asf are portion, ring, bar, strip, section and area sampling fractions, respectively, and $\Sigma Q^-/2$ is the total number of particles counted using two-way physical disectors.

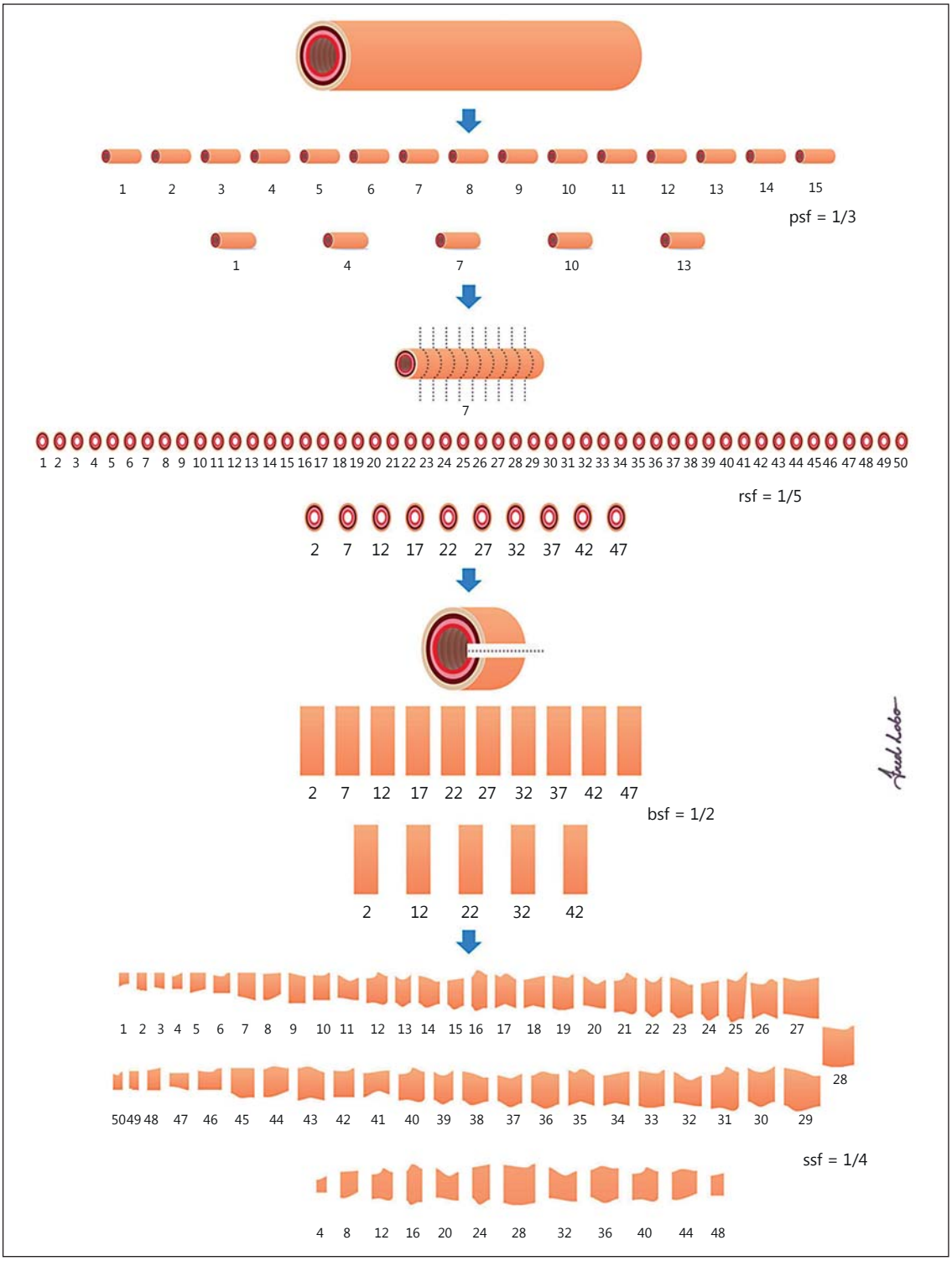

Color version available online

Fig. 1. Schematic drawing depicting the SUR sampling of a healthy horse ileum. Initially, each ileum was sectioned into fifteen 3-cm-thick portions. A sampling fraction of these portions (psf = 1/3) was chosen. Subsequently, each of these 5 portions was then divided into ten 0.3-cm-thick rings, and a sampling fraction of these rings (rsf = 1/5) was selected obtaining 10 rings on average, which were opened and arranged into bars. A sampling fraction of these bars (bsf = 1/2) was selected generating on average 5 bars. Next step, each bar was cut into 10 strips, on average, and arranged in order of increasing size using the smooth fractionator principle. Finally, a sampling fraction of these strips (ssf = 1/4) – on average 12 strips per ileum – were sampled for embedding.

Mean Volume of Myenteric and Submucosal Neurons

The mean perikaryal volume of myenteric or submucosal neurons was estimated by the nucleator method [Gundersen, 1988] using the 4 half-line nucleator probe available in the newCAST Visiopharm stereology system and in the same reference sections used for total number estimation. Nucleoli were sampled using one 2-µm- and one 0.6-µm-thick section in a physical disector. The following formula was used to estimate the mean perikaryal volume:

$$\bar{v}_{N\ mye/sub} = \Sigma(4\pi/3) \cdot \bar{l}_n^3,$$

where $\bar{v}_{N\ mye/sub}$ is the mean volume of myenteric and submucosal neurons and $\bar{l}_n^3$ is the mean of all cubed distances from a central point (nucleolus) within the perikaryon to its cell boundaries.

Total Volume of Ileum Layers

Fractional ileum volumes occupied by the muscular (circular + longitudinal strata) and submucosal layers of the ileum were estimated by applying lattices of test points to VUR images [Howard and Reed, 2010]. The total volumes of ileums occupied by the muscular and submucosal layers were obtained by multiplying volume fractions by corresponding ileum volumes.

Statistical Analyses

The precision of a stereological estimate was expressed as a coefficient of error (CE) calculated as described by Gundersen et al. [1999]. Stereological data were expressed as group mean (observed CV), where the observed CV represents the SD/mean. Group differences were assessed by the non-parametric Mann-Whitney test using SAS version 9.2 statistical software. Null hypotheses were rejected when the probability level for apparent differences was $p < 0.05$.

Results

Genetic Diagnosis of ICA

RT-PCR depicted that all foals from the ICA group were homozygous for the mutant form of the allele Lys 118 of the EDNRB gene – responsible for OLWS – whilst their parents were heterozygous. In addition, all foals (and their parents) from the healthy group were homozygous wild-type for the allele Ile 118 of the EDNRB gene.

Clinical Examination

All foals received colostrum and showed a good appetite. Animals from the ICA group had a white coat with blue irises and three of them had black spots around the mouth. Their behaviour was normal. However, 18 h after birth, on average, the ICA animals showed signs of recurring abdominal discomfort and abdominal pain (fig. 2) with a decrease in intestinal motility (hypomotility) – or absence of it – and tenesmus. Other symptoms observed were: hyporexia, tachypnea and tachycardia. Animals received 1.1 mg·kg^{-1} intravenous flunixin meglumine for 3–6 days, but they were euthanized after that period since the therapy was ineffective. Healthy foals had no clinical signs of gastrointestinal disorders and their intestinal motility was normal.

Color version available online

Fig. 2. Image of an overo white body-spot ICA foal, 18 h after birth, showing signs of recurring abdominal discomfort and abdominal pain.

Structure of Myenteric and Submucosal Ganglia

Myenteric Ganglia

The ileum myenteric ganglia of the healthy group were situated between the two strata – circular and longitudinal – of the muscular layer. The ganglia were connective tissue encapsulated and predominantly elongated containing, on average, two or three layers of nerve cells. In addition, neurons could be scattered with no connective sheath. Myenteric neurons were uninucleate, with their nuclei located either centrally or eccentrically (fig. 3A). In contrast, the structure of myenteric ganglia from 2 ICA animals was starkly modified, i.e. ganglia were oval or irregular in shape, non-encapsulated and contained neurons with vacuoles alongside glial cells (fig. 3B). In 3 animals from the ICA group, no myenteric ganglia (and myenteric neurons) were observed and the two strata – circular and longitudinal – of the muscular layer were quite adjacent and intertwined in some portions of the ileum wall (fig. 3C).

Submucosal Ganglia

In the healthy horses, the submucosal ganglia were located in the submucosal layer of the ileum. According to the position of the ganglia, two submucosal plexuses were

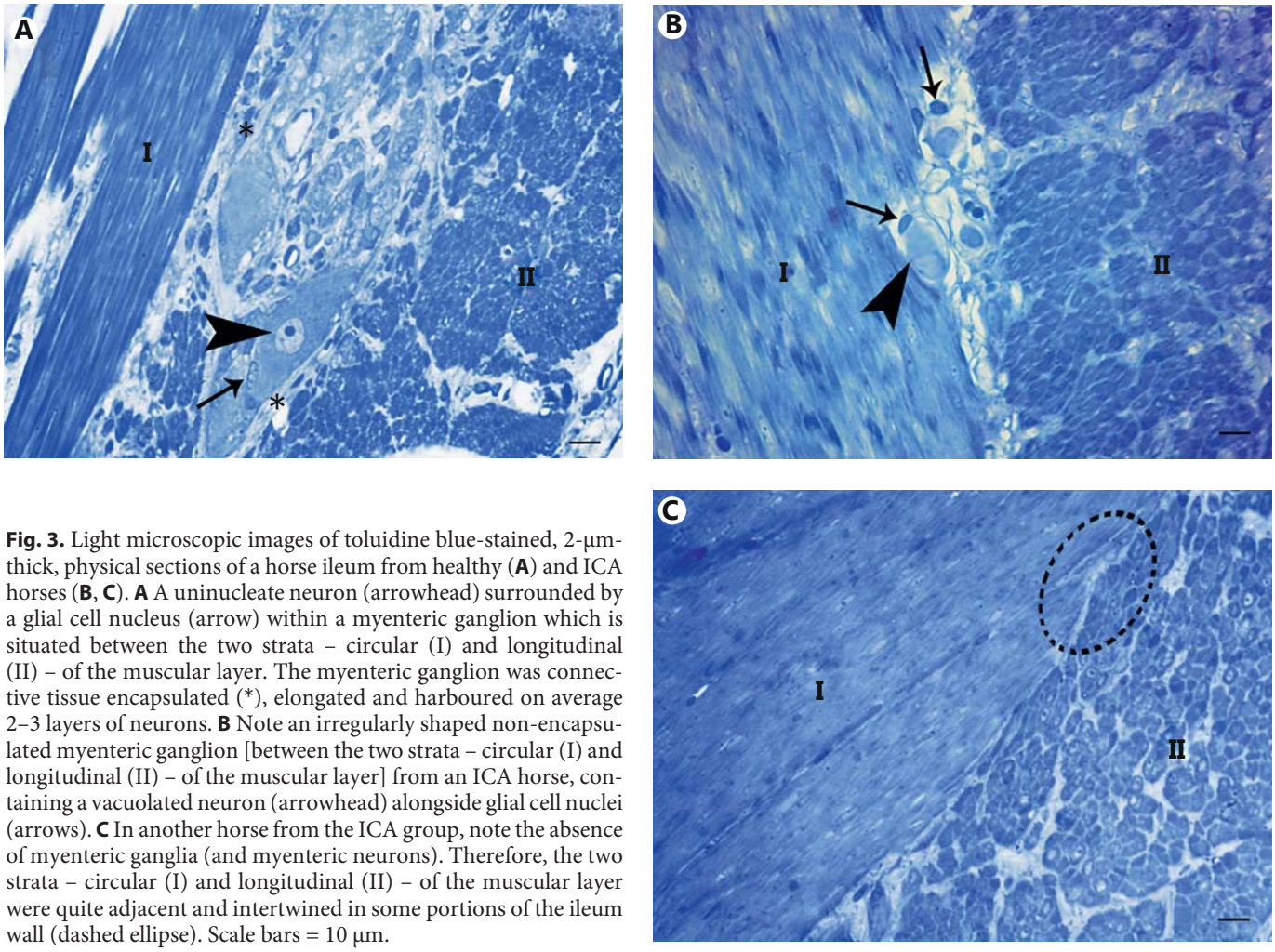

Fig. 3. Light microscopic images of toluidine blue-stained, 2-µm-thick, physical sections of a horse ileum from healthy (**A**) and ICA horses (**B**, **C**). **A** A uninucleate neuron (arrowhead) surrounded by a glial cell nucleus (arrow) within a myenteric ganglion which is situated between the two strata – circular (I) and longitudinal (II) – of the muscular layer. The myenteric ganglion was connective tissue encapsulated (*), elongated and harboured on average 2–3 layers of neurons. **B** Note an irregularly shaped non-encapsulated myenteric ganglion [between the two strata – circular (I) and longitudinal (II) – of the muscular layer] from an ICA horse, containing a vacuolated neuron (arrowhead) alongside glial cell nuclei (arrows). **C** In another horse from the ICA group, note the absence of myenteric ganglia (and myenteric neurons). Therefore, the two strata – circular (I) and longitudinal (II) – of the muscular layer were quite adjacent and intertwined in some portions of the ileum wall (dashed ellipse). Scale bars = 10 µm.

Table 1. Ileum volume (cm^3) and total volumes of muscular (circular + longitudinal) and submucosal ileum layers (cm^3), total number of myenteric and submucosal neurons, and mean volume of myenteric and submucosal neurons (μm^3) in healthy and ICA horses

Stereological parameters	Healthy	ICA
Volume		
Ileum^{NS1}	178.5 (0.37)	67.8 (0.23)
Muscular layer^{NS2}	58.8 (0.47)	26 (0.13)
Submucosal layer^{NS3}	65 (0.37)	19.6 (0.42)
Total number of myenteric neurons*	46,376,456 (0.27)	259,428 (0.55)
Total number of submucosal neurons**	16,436,182 (0.24)	0
Mean volume of myenteric neurons***	2,574 (0.36)	932 (0.26)
Mean volume of submucosal neurons****	2,275 (0.26)	0

Values are group means, with CVs in parentheses. Means that share a letter are not significantly different (^{NS}). ^{NS1} p = 0.189; ^{NS2} p = 0.191; ^{NS3} p = 0.277.

Means that do not share a letter are significantly different (*). * p = 0.0112; ** p = 0.0075; *** p = 0.0112; **** p = 0.0075.

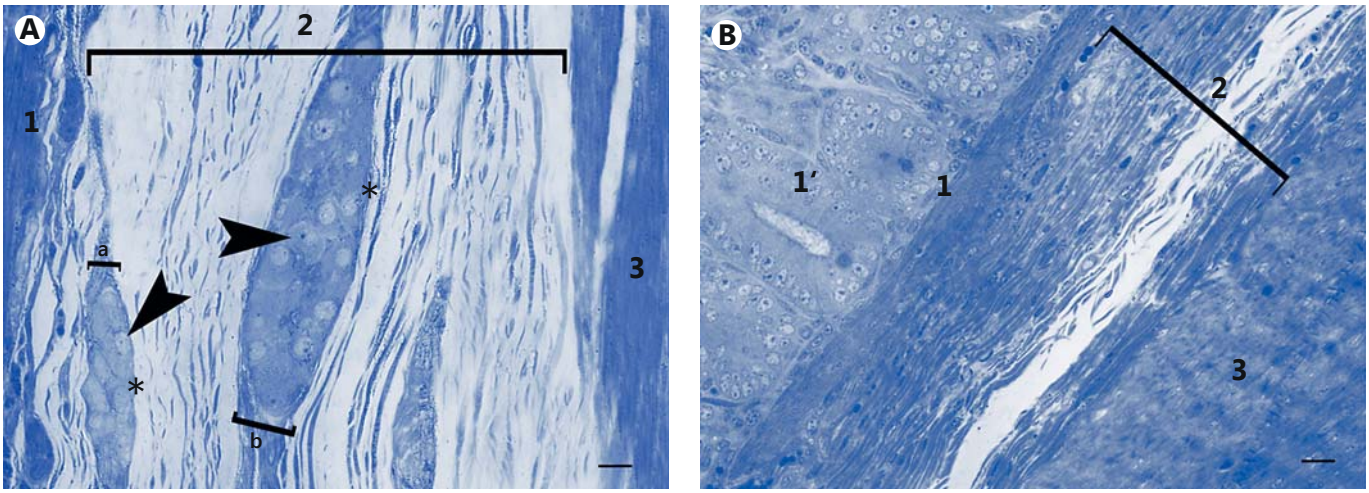

Fig. 4. Light microscopic images of toluidine blue-stained, 2-μm-thick, physical sections of a horse ileum from healthy (**A**) and ICA horses (**B**). **A** In healthy horses, two submucosal plexuses were observed immersed in the submucosal ileum layer (2): the internal submucosal plexus (a), adjacent to the mucosal layer (1), and the external submucosal plexus (b), close to the inner part of the circular stratum of the muscular layer (3). In the internal submucosal plexus (a), neurons were arranged in two layers (arrowhead), heterogeneously distributed and formed elongated connective tissue encapsulated (*) or non-encapsulated ganglia. In the external submucosal plexus (b), neurons were homogeneously distributed and formed elongated connective tissue-encapsulated ganglia (*) containing, on average, two or three layers of neurons (arrowhead). **B** The ICA horses presented neither submucosal ganglia and submucosal neurons nor glial cells immersed in the submucosal ileum layer (2). No ectopic submucosal neurons were found in the immediate vicinity of the mucosal layer (1, 1') nor close to the inner part of the circular stratum of the muscular layer (3). Scale bars = 20 μm.

observed: external and internal submucosal plexuses. The external submucosal plexus was positioned close to the inner part of the circular stratum of the muscular layer, whereas the internal submucosal plexus was adjacent to the ileum mucosal layer. In the external submucosal plexus, neurons were homogeneously distributed and formed elongated connective tissue-encapsulated ganglia containing, on average, two or three layers of nerve cells (fig. 4A).

However, in the internal submucosal plexus, neurons were arranged in two layers, heterogeneously distributed and formed elongated connective tissue-encapsulated or non-encapsulated ganglia. Glial cells were observed in both plexuses (fig. 4A).

In stark contrast, ICA horses presented neither submucosal ganglia and submucosal neurons nor glial cells immersed in the submucosal ileum layer. No ectopic submucosal neurons were found in the immediate vicinity of the mucosal layer nor close to the inner part of the circular stratum of the muscular layer (fig. 4B).

Volume of Ileum

The stereological data were collated in form of a table (table 1).

The volume of the ileum amounted to 178.5 cm^3 (CV 0.37) in the healthy group and 67.8 cm^3 (CV 0.23) in the ICA group. Apparent inter-group differences were not significant ($p = 0.189$; table 1). The precision of estimated ileum volume [expressed as $CE(V_{ILE})$] was 0.03 for the healthy group and 0.02 for the ICA group.

Total Number of Myenteric and Submucosal Neurons

The total number of myenteric neurons was 46,376,456 (CV 0.27) for the healthy group and 259,428 (CV 0.55) for the ICA group. Of the 5 ICA animals studied, only 2 foals presented myenteric neurons and 3 foals had no myenteric neurons at all. Between-group differences were significant ($p = 0.0112$; table 1). The precision of the estimated number of myenteric neurons [expressed as $CE(N_{mye})$] was 0.03 for the healthy group and 0.02 for the ICA group.

The total number of submucosal neurons was 16,436,182 (CV 0.24) for the healthy group and nil for the ICA group. Of the 5 ICA animals studied, none presented submucosal neurons. Between-group differences were significant ($p = 0.0075$; table 1). The precision of the estimated number of submucosal neurons [expressed as $CE(N_{sub})$] was 0.03 for the healthy group and 0 for the ICA group.

Mean Volume of Myenteric and Submucosal Neurons

The mean perikaryal volume of myenteric neurons was 2,574 μm^3 (CV 0.36) for the healthy group and 932 μm^3 (CV 0.26) for the ICA group. Between-group differences were significant ($p = 0.0112$; table 1).

The mean perikaryal volume of submucosal neurons was 2,275 μm^3 (CV 0.26) for the healthy group and nil for the ICA group. Between-group differences were significant ($p = 0.0075$; table 1).

Total Volume of Ileum Layers

The fractional volume of ileum occupied by the muscular (circular + longitudinal strata) layer amounted to 0.365 (CV 0.18) in the healthy group and 0.383 (CV 0.13) in the ICA group. Inter-group differences were not significant ($p = 0.639$). The total volume of the muscular (circular + longitudinal strata) layer was 58.8 cm^3 (CV 0.47) in the healthy group and 26 cm^3 (CV 0.13) in the ICA group. Apparent between-group differences were not significant ($p = 0.191$; table 1).

The fractional volume of ileum occupied by the submucosal layer amounted to 0.3163 (CV 0.21) in the healthy group and 0.2891 (CV 0.42) in the ICA group. Inter-group differences were not significant ($p = 0.680$). The total volume of the submucosal layer was 65 cm^3 (CV 0.37) in the healthy group and 19.6 cm^3 (CV 0.42) in the ICA group. The apparent between-group differences were not significant ($p = 0.277$; table 1).

Discussion

In this study, 3-D technology, i.e. design-based stereology, was used to study the gut of horses with ICA. This technology helped us understand the structural problems of this disease more precisely.

The most startling finding of this study was just how powerful this disease is. Of the two groups of neurons found in the gut – myenteric and submucosal – there was a 99% decrease in myenteric neurons, and absolutely no submucosal neurons were left in the sick animals. The remaining neurons were reduced to more than half the size, with a 63.8% decrease in volume, i.e. atrophy.

Our results differed substantially from previous respectable studies in number and size of enteric neurons in healthy horses. For example, in his study, Pearson [1994] reported on average 25 neuron profiles per ganglion in the external or internal submucosal plexuses of the jejunum. Pearson [1994] sampled about 135 ganglia in each submucosal plexus, which would give an average of 3,375 neuron profiles. Our estimate for the amount of neurons in the ileum submucosal plexus is as many as 2,434-fold higher.

Another study conducted on the ileum of healthy horses by Doxey et al. [1995] estimated the number of neuron profiles in the myenteric and submucosal plexuses of horses as 8,808 and 14,352, respectively. Again, our estimates for the horse ileum were 5,264- and 1,144-fold higher, respectively. In the most recent study, Freytag et al. [2008] reported 58,400 myenteric neuron profiles per cm^2 of jejunum ganglion area in healthy horses, whereas our results were not in the thousands but millions, i.e. 46,376,456. These results, we strongly believe, are important for developments in gene therapy.

Yet another difference in those previous studies relates to how they calculated the size of the cells. Both Freytag et al. [2008] and Burns and Cummings [1991] assumed that they could estimate the size of a myenteric neuron by measuring its profile area. However, since cells are 3-D particles, the true size of them is morphologically estimated by measuring their volume [Gundersen, 1988; Howard and Reed, 2010], as we did in this paper.

Our findings are a step forward from previous results because of our new use of 3-D technology. The discrepancies between our estimates and the ones from Burns and Cummings [1991], Pearson [1994], Doxey et al. [1995] and Freytag et al. [2008] are due to the fact that those authors used 2-D sampling and 2-D counting methods. Although those previous studies had their importance in the past, they could not estimate the total number or the volumetric size of enteric neurons in the whole horse jejunum or ileum but the number of neuron profiles per intestinal segment area or the area of a given neuron profile.

These discrepancies confirm the danger of coming to conclusions based only upon ratios, without sampling the whole reference space as we were able to do in this study using design-based stereology. This is a well-known problem when using linear or areal measurement methods – a pitfall known as reference trap [Hunziker and Cruz-Orive, 1986; Cruz-Orive, 1994]. Because of these different methodological approaches, the estimates by Burns and Cummings [1991], Pearson [1994], Doxey et al. [1995] and Freytag et al. [2008] cannot be directly compared to our data. Our unit measurements cannot be reconciled: the cell sizes in this study were measured in cubic micrometres, whereas previous studies used square and linear metric units.

More importantly, after systematically reviewing the literature, we were unable to find 2-D or 3-D quantitative studies on the structure (number and size) of enteric neu-

rons in horses with ICA. To the best of our knowledge, this is the first time that design-based stereology has been used to describe the quantitative structure of the enteric nervous system of ICA horses.

Concluding Remarks and Future Research Directions

We believe that this study forms the structural basis for further research which may assess which subpopulation of myenteric neurons are affected by ICA.

In addition, our findings in this field suggest using the term 'aganglionosis' specifically for submucosal neurons. When we use the term 'aganglionosis', we mean that there are no neurons left in the gut. However, we found myenteric neurons in 2 out of 5 diseased horses. Because of this, we would like to propose a new nomenclature to distinguish between a complete absence of neurons – aganglionosis – and a weaker form of the disease which we suggest naming 'hypoganglionosis'.

Our results are a step forward in understanding this disease structurally. It cannot be cured but pharmaceutical companies may be able to use these findings to devise specific gene therapy strategies for either preventing the illness ever occurring or treating the disease in the horse, which is a naturally occurring model for studying Hirschsprung's disease in humans.

Acknowledgments

The Laboratory of Stochastic Stereology and Chemical Anatomy is supported by São Paulo Research Foundation (application No. 2007/50168-4). The authors also thank Frederico Jorge Lobo Ladd for producing figure 1.

References

Baddeley, A.J., H.J.G. Gundersen, H.J.G. Cruz-Orive (1986) Estimation of surface area from vertical sections. J Microsc *142:* 259–276.

Brashier, M.K., R.J. Geor (1995) Gastrointestinal diseases of the neonate; in Kobluk, C., T.R. Ames, R.J. Geor: The Horse. Diseases and Clinical Managment. Philadelphia, Saunders, pp 55–1237.

Burns, G.A., J.F. Cummings (1991) Equine myenteric plexus with special reference to the pelvic flexure pace-maker. Anat Rec *230:* 417–424.

Cruz-Orive, L.M. (1994) Toward a more objective biology. Neurobiol Aging *15:* 377–378.

Doxey, D.L., G.T. Pearson, E.M. Milne, J.S. Gilmour, H.K. Chisholm (1995) The equine enteric nervous system – neuron characterization and distribution in adults and juveniles. Vet Res Commun *19:* 433–449.

Finno, C.J., S.J. Spier, S.J. Valberg (2009) Equine diseases caused by known genetic mutations. Vet J *179:* 336–347.

Freytag, C., J. Seeger, T. Siegemund, J. Grosche, A. Grosche, D.E. Freeman, G.F. Schusser, W. Härtig (2008) Immunohistochemical characterization and quantitative analysis of neurons in the myenteric plexus of the equine intestine. Brain Res *1244:* 53–64.

Gundersen, H.J.G. (1977) Notes of the estimation of the numerical density of arbitrary profiles: the edge effect. J Microsc *111:* 219–223.

Gundersen, H.J.G. (1986) Stereology of arbitrary particles. A review of unbiased number and size estimators and the presentation of some new ones, in memory of William R. Thompson. J Microsc *143:* 3–45.

Gundersen, H.J.G. (1988) The nucleator. J Microsc *151:* 3–21.

Gundersen, H.J.G. (2002) The smooth fractionator. J Microsc *207:* 191–210.

Gundersen, H.J.G., F.B. Jensen, K. Kieu, J. Nielsen (1999) The efficiency of systematic sampling in stereology – reconsidered. J Microsc *193:* 199–211.

Howard, C.V., M.G. Reed (2010) Unbiased Stereology. Three-Dimensional Measurement in Microscopy. Liverpool, QTP Publications, pp 39–56.

Hultgren, B.D. (1982) Ileocolonic aganglionosis in white progeny of overo spotted horses. J Am Vet Med Assoc *180:* 289–292.

Hunziker, E.B., L.M. Cruz-Orive (1986) Consistent and efficient delineation of reference spaces for light microscopical stereology using a laser microbeam system. J Microsc *142:* 95–99.

Kissmeyer-Nielsen, P., H. Christensen, S. Laurberg (1994) Diverting colostomy induces mucosal and muscular atrophy in rat distal colon. Gut *35:* 1275–1281.

Lightbody, T. (2002) Foal with overo lethal white syndrome born to a registered quarter horse mare. Can Vet J *43:* 715–717.

Mayhew, T.M. (1991) The accurate prediction of Purkinje cell number from cerebellar weight can be achieved with the fractionator. J Comp Neurol *308:* 162–168.

McCabe, L., L.D. Griffin, A. Kinzer, M. Chandler, J.B. Beckwith, E.R.B. McCabe (1990) Overo lethal white foal syndrome: equine model of aganglionic megacolon (Hirschsprung disease). Am J Med Genet *36:* 336–340.

Metallinos, D.L., A.T. Bowling, J. Rine (1998) A missense mutation in the endothelin-B receptor gene is associated with lethal white foal syndrome: an equine version of Hirschsprung disease. Mamm Genome *9:* 426–431.

Nagahama, M., R. Semba, M. Tsuzuki, T. Ozaki (2001) Distribution of peripheral nerve terminals in the small and large intestine of congenital aganglionosis rats (Hirschsprung's disease rats). Pathol Int *51:* 145–157.

Ogiolda, L., R. Wanke, O. Rottmann, W. Hermanns, E. Wolf (1998) Intestinal dimensions of mice divergently selected for body weight. Anat Rec *250:* 292–299.

Okamoto, E., T. Ueda (1967) Embryogenesis of intramural ganglia of the gut and its relation to Hirschsprung's disease. J Pediatr Surg *2:* 437–443.

Parry, N.M.A. (2005) Overo lethal white foal syndrome. Comp Contin Edu Pract Vet *27:* 945–950

Pearson, G.T. (1994) Structural organization and neuropeptide distributions in the equine enteric nervous system: an immunohistochemical study using whole-mount preparations from the small intestine. Cell Tissue Res *276:* 523–534.

Santschi, E.M., A.K. Purdy, S.J. Valberg, P.D. Vrotsos, H. Kaese, J.R. Mickelson (1998) Endothelin receptor B polymorphism associated with lethal white foal syndrome in horses. Mamm Genome *9:* 306–309.

SAS (2008): SAS/STAT 9.2 User's Guide. Cary, SAS Institute, p 584.

Schmittgen, T.D., K.J. Livak (2008) Analyzing real-time PCR data by the comparative C(T) method. Nat Protoc *3:* 1101–1108.

Taniguchi, K., K. Matsuura, T. Matsuoka, H. Nakatani, T. Nakano, Y. Furuya, T. Sugimoto, M. Kobayashi, K. Araki (2005) A morphological study of the pacemaker cells of the aganglionic intestine in Hirschsprung's disease utilizing ls/ls model mice. Med Mol Morphol *38:* 123–129.

Vonderfecht, S.L, A.T. Bowling, M. Cohen (1983) Congenital intestinal aganglionosis in white foals. Vet Pathol *20:* 65–70.

Weibel, E.R. (1979) Stereological Methods. Practical Methods for Biological Morphometry. London, Academic Press, vol 1, pp 21–415.